J|A|C|S
ARTICLES
Published on Web 11/28/2002

Insights into the Metathesis Reaction Involving M−M, C−C, and M−C Triple Bonds from Computations Employing Density Functional Theory on Model Compounds $M_2(OH)_6$ and $M_2(SH)_6$, Where M = Mo and W

Malcolm H. Chisholm,*,† Ernest R. Davidson,*,‡ and Kristine B. Quinlan§

Contribution from the Department of Chemistry, The Ohio State University, 100 West 18th Avenue, Columbus, Ohio 43085, Department of Chemistry, University of Washington, Box 351700, Seattle, Washington 98195-1700, and Department of Chemistry, Indiana University, 800 East Kirkwood Avenue, Bloomington, Indiana 47405

Received June 17, 2002

Abstract: Calculations employing density functional theory (Gaussian 98, B3LYP, LANL2DZ, 6-31G*) have been undertaken to interrogate the factors influencing the metathesis reaction involving M−M, C−C, and M−C triple bonds for the model compounds $M_2(EH)_6$, $M_2(EH)_6(\mu\text{-}C_2H_2)$, and $[(HE)_3M(\equiv CH)]_2$, where M = Mo, W and E = O, S. Whereas in all cases the ethyne adducts are predicted to be enthalpically favored in the reactions between $M_2(EH)_6$ compounds and ethyne, only when M = W and E = O is the alkylidyne product $[(HO)_3W(\equiv CH)]_2$ predicted to be more stable than the alkyne adduct. For the reaction $M_2(EH)_6(\mu\text{-}C_2H_2) \rightarrow [(HE)_3M(\equiv CH)]_2$, the $\Delta G°$ values (kcal mol^{-1}) are −6 (M = W, E = O), +5 (M = Mo, E = O), +18 (M = W, E = S), and +21 (M = Mo, E = S) and the free energies of activation are calculated to be $\Delta G^{\ddagger}$ = +19 kcal mol^{-1} (M = W, E = O) and +34 kcal mol^{-1} (M = Mo, E = O), where the transition state involves an asymmetric bridged structure $M_2(OH)_4(\mu\text{-}OH)_2(CH)(\mu\text{-}CH)$ in which the C−C bond has broken; C···C = 1.89 and 1.98 Å for W and Mo, respectively. These results are discussed in terms of the experimental observations of the reactions involving ethyne and the symmetrically substituted alkynes (RCCR, where R = Me, Et) with $M_2(O^tBu)_6$ and $M_2(O^tBu)_2(S^tBu)_4$ compounds, where M = Mo, W.

Introduction

Olefin and alkyne metathesis reactions have attracted considerable preparative and theoretical interest. Indeed, largely through the efforts of Schrock,[1] Grubbs,[2] and subsequently others,[3] the metal-carbene/alkylidene mediated olefin metathesis reaction has emerged as one of the most important reactions in metal mediated preparative procedures. Certainly, ring-closure metathesis, RCM, and ring-opening polymerization metathesis, ROMP, are now well-established and commonly employed procedures in modern day organic and polymer synthesis. Somewhat related but less well studied reactions involving M−M and C−C multiple bonds are shown schematically in eqs 1 and 2 below.

$$[M{=}M] + [C{=}C] \rightleftharpoons 2[M{=}C] \qquad (1)$$

$$[M{\equiv}M] + [C{\equiv}C] \rightleftharpoons 2[M{\equiv}C] \qquad (2)$$

Certain early transition metal alkylidene complexes are known to decompose by bimolecular pathways yielding alkenes, but there does not seem to be any bona fide example of eq 1 to date. The forward reaction involving the mutual scission of M−M and C−C triple bonds, the "chop-chop reaction", was first noted by Schrock 20 years ago in the reactions between certain alkynes and $W_2(O^tBu)_6$, eq 3.

$$W_2(O^tBu)_6 + RC{\equiv}CR \rightarrow 2[(^tBuO)_3W{\equiv}CR] \qquad (3)$$

A variation on the reaction shown in eq 3 involving terminal alkynes was subsequently developed as a simple route to $(^tBuO)_3W{\equiv}CR$ compounds which are commonly employed as alkyne metathesis catalysts (e.g., R = ^{t}Bu).[4]

The reaction shown in eq 3 is very sensitive to the selection of specific alkoxide or aryloxide ligands. The introduction of trialkylsiloxide ligands as in $W_2(OSiMe^tBu_2)_6$[5] or thiolates in $W_2(O^tBu)_2(S^tBu)_4$[6] completely shuts down the metathesis reaction. Moreover, the related molybdenum compound $Mo_2(O^tBu)_6$

* Address correspondence to these authors. E-mail: chisholm@chemistry.ohio-state.edu, erdavid@u.washington.edu.
† The Ohio State University.
‡ University of Washington.
§ Indiana University.

(1) (a) Schrock, R. R. *Polyhedron* **1995**, *14*, 3177. (b) Schrock, R. R. *Acc. Chem. Res.* **1990**, *23*, 158; (c) Schrock, R. R.; Freudenberger, J. H.; Listemann, M. L.; McCullough, L. G. *J. Mol. Catal.* **1985**, *28*, 1.
(2) (a) Trnka, T. M.; Grubbs, R. H. *Acc. Chem. Res.* **2001**, *34*, 18. (b) Grubbs, R. H.; Chang, S. *Tetrahedron* **1998**, *54*, 4413.
(3) (a) Fürstner, A. *Angew. Chem., Int. Ed.* **2000**, *39*, 3012. (b) Ge, P.-H.; Fu, W.; Herrmann, W. A.; Herdtweck, E.; Campana, C.; Adams, R. D.; Bunz, U. H. F. *Angew. Chem., Int. Ed.* **2000**, *39*, 3607. (c) Weskamp, T.; Kohl, F. J.; Hieringer, W.; Gleich, D.; Herrmann, W. A. *Angew. Chem., Int. Ed.* **1999**, *38*, 2416.
(4) Schrock, R. R.; Listemann, M. L.; Strugeoff, L. G. *J. Am. Chem. Soc.* **1982**, *104*, 4291.
(5) Chisholm, M. H.; Cook, C. M.; Folting, K.; Streib, W. E. *Inorg. Chim. Acta* **1992** *198*−*200*, 63.

does not react with RC≡CR (R = Me, Et, Pr^n) in an analogous manner, though certain (^{t}BuO)$_3$Mo≡CR compounds have been prepared from related reactions employing terminal alkynes.[7] In work in our laboratory, we had observed the formation of alkyne adducts in a variety of reactions employing $M_2(OR)_6$ compounds, where M = Mo and W and R = ^{t}Bu, ^{i}Pr, and $CH_2{}^t$Bu. In certain cases, we also found evidence for an equilibrium involving the alkyne adducts and the alkylidyne complexes, eq 4, but only when the metal was tungsten.[8]

$$W_2(O^tBu)_6(\mu\text{-}C_2R_2) \rightleftharpoons 2[(^tBuO)_3W{\equiv}CR] \qquad (4)$$

A simple verification of this statement is seen in the reactions involving the alkyne adduct formed from $H^{13}C^{13}CH$ and DCCD. In the case of tungsten, the alkylidyne species (^{t}BuO)$_3$W≡^{13}CH and (^{t}BuO)$_3$W≡CD can be detected along with the alkyne adduct $W_2(O^tBu)_6(\mu\text{-}H^{13}CCD)$ formed from their coupling. The related molybdenum compounds are not similarly formed from the kinetically labile but from otherwise well-characterized ethyne adducts of $Mo_2(O^tBu)_6$.[9] With the advent of modern computational methods employing density functional theory and the ready availability of programs such as Gaussian 98,[10] it is possible to interrogate the fundamental thermodynamic and kinetic factors that are controlling these reactions. We describe here our investigations of the reactions between ethyne and the model compounds $M_2(EH)_6$ (M≡M), where M = Mo and W and E = O and S. Though the use of OH and SH to model ^{t}BuO and ^{t}BuS is clearly a significant approximation, the findings are particularly enlightening with regard to the experimental observations and the calculated free energies are proposed to duplicate the trends in reactivity. The results reported here are also particularly relevant to recent findings concerning the reductive cleavage of dinitrogen to give 2 equiv of a metal nitride[11] and its reverse reaction wherein homo or heterometallic metal nitride complexes react to either form bridged dinitrogen complexes or undergo reduction with the expulsion of N_2.[12]

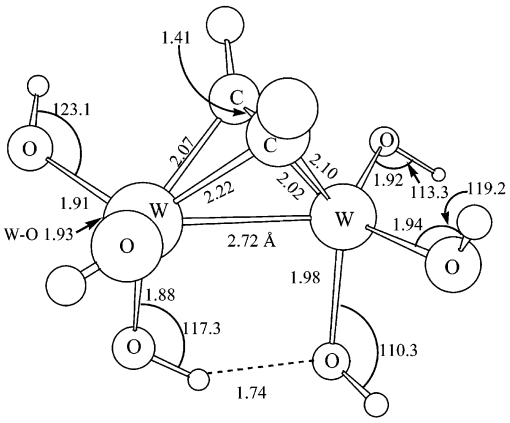

Figure 1. Optimized structure of $W_2(OH)_6(\mu\text{-}C_2H_2)$ with terminal OH groups with selected bond lengths (Å) and angles (deg).

Results and Discussion

Calculated Reaction Thermodynamics. To extend our understanding of the alkyne-cleavage reaction, the thermodynamics of the reactions shown in eq 5, for M = Mo, W and E = O, S, were first calculated using density functional theory.

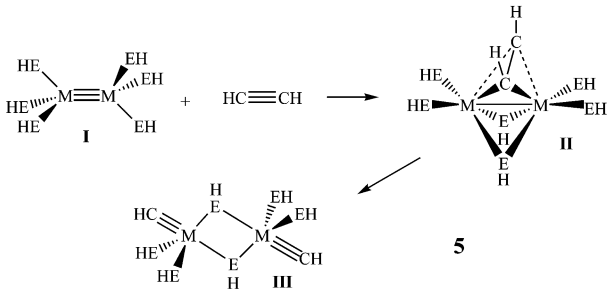

Calculations have been done previously on the model compounds $M_2(OH)_6$ (**I**).[6,13] Structural parameters from the X-ray data for $W_2(O^iPr)_6(py)_2(\mu\text{-}C_2H_2)$[8] were used as a starting point for the geometry optimizations of **II**. The pyridine ligands were omitted, and EH was substituted for O^{i}Pr. This geometry is also very similar to the structure of $M_2(O^tBu)_6(\mu\text{-CO})$, which has two bridging and four terminal alkoxides.[14] For M = W, $W_2(OH)_6(\mu\text{-}C_2H_2)$ was also optimized with all terminal hydroxides, which resulted in an internal hydrogen bond, as shown in Figure 1, and an energy essentially equivalent to that of the doubly bridged species. The similarity in energies of the bridged and unbridged structures seemingly correlates well with the observation that the molecules $M_2(O^tBu)_6(\mu\text{-CO})$[14] are fluxional on the NMR time scale and not frozen out in a bridged form, even at −80 °C in toluene-d_8 (M = Mo or W).

The cleaved product (**III**) was modeled with EH groups bridging the two halves of the molecule, as is seen in the crystal

(6) Chisholm, M. H.; Davidson, E. R.; Huffman, J. C.; Quinlan, K. B. *J. Am. Chem. Soc.* **2001**, *123*, 9652.
(7) Strutz, H.; Schrock, R. R. *Organometallics* **1984**, *3*, 1600.
(8) (a) Chisholm, M. H.; Folting, K.; Hoffman, D. M.; Huffman, J. C. *J. Am. Chem. Soc.* **1984**, *106*, 6794. (b) Chisholm, M. H.; Conroy, B. K.; Huffman, J. C.; Marchant, N. S. *Angew. Chem., Int. Ed. Engl.* **1986**, *25*, 446. (c) Chisholm, M. H.; Folting, K.; Huffman, J. C.; Lucas, E. A. **1991**, *10*, 535.
(9) (a) Chisholm, M. H.; Folting, K.; Huffman, J. C.; Rothwell, I. D. *J. Am. Chem. Soc.* **1982**, *104*, 4389. (b) Chisholm, M. H.; Hoffman, D. M.; McCandless, J. N.; Huffman, J. C. *Polyhedron* **1997**, *16*, 839.
(10) Frisch, M. J.; Trucks, G. W.; Schlegel, H. B.; Scuseria, G. E.; Robb, M. A.; Cheeseman, J. R.; Zakrzewski, V. G.; Montgomery, J. A., Jr.; Stratmann, R. E.; Burant, J. C.; Dapprich, S.; Millam, J. M.; Daniels, A. D.; Kudin, K. N.; Strain, M. C.; Farkas, O.; Tomasi, J.; Barone, V.; Cossi, M.; Cammi, R.; Mennucci, B.; Pomelli, C.; Adamo, C.; Clifford, S.; Ochterski, J.; Petersson, G. A.; Ayala, P. Y.; Cui, Q.; Morokuma, K.; Malick, D. K.; Rabuck, A. D.; Raghavachari, K.; Foresman, J. B.; Cioslowski, J.; Ortiz, J. V.; Stefanov, B. B.; Liu, G.; Liashenko, A.; Piskorz, P.; Komaromi, I.; Gomperts, R.; Martin, R. L.; Fox, D. J.; Keith, T.; Al-Laham, M. A.; Peng, C. Y.; Nanayakkara, A.; Gonzalez, C.; Challacombe, M.; Gill, P. M. W.; Johnson, B.; Chen, W.; Wong, M. W.; Andres, J. L.; Gonzalez, C.; Head-Gordon, M.; Replogle, E. S.; Pople, J. A. *Gaussian 98*, revision A.6; Gaussian, Inc.: Pittsburgh, PA, 1998.
(11) (a) Laplaza, C. E.; Cummins, C. C. *Science* **1995**, *268*, 861. (b) Laplaza, C. E.; Johnson, M. J. A.; Peters, J. C.; Odom, A. L.; Kim, E.; Cummins, C. C.; George, G. N.; Pickering, I. J. *J. Am. Chem. Soc.* **1996**, *118*, 8623. (c) Laplaza, C. E.; Johnson, A. R.; Cummins, C. C. *J. Am. Chem. Soc.* **1996**, *118*, 709. (d) Tsai, Y.-C.; Johnson, M. J. A.; Mindiola, D. J.; Cummins, C. C.; Klooster, W. T.; Koetzle, T. F. *J. Am. Chem. Soc.* **1999**, *121*, 10426. (e) Mindiola, D. J.; Meyer, K.; Cherry, J.-P. F.; Baker, T. A.; Cummins, C. C. *Organometallics* **2000**, *19*, 1622. (f) Caselli, A.; Solari, E.; Scopelliti, R.; Floriani, C.; Re, N.; Rizzoli, C.; Chiesi-Villa, A. *J. Am. Chem. Soc.* **2000**, *122*, 3652.
(12) (a) Seymore, S. B.; Brown, S. N. *Inorg. Chem.* **2002**, *41*, 462. (b) Ware, D. C.; Taube, H. *Inorg. Chem.* **1991**, *30*, 4605. (c) Lam, H. W.; Che, C. M.; Wong, K. Y. *J. Chem. Soc., Dalton Trans.* **1992**, 1411. (d) Demadis, K. D.; El-Samanody, E.-S.; Coia, G. M.; Meyer, T. J. *J. Am. Chem. Soc.* **1999**, *121*, 535. (e) Newton, C.; Edwards, K. D.; Ziller, J. W.; Doherty, N. M. *Inorg. Chem.* **1999**, *38*, 4032.
(13) (a) Cotton, F. A.; Stanley, G. G.; Kalbacher, B. J.; Green, J. C.; Seddon, E.; Chisholm, M. H. *Proc. Natl. Acad. Sci. U.S.A.* **1997**, *74*, 3109. (b) Bursten, B. E.; Cotton, F. A.; Green, J. C.; Seddon, E.; Stanley, G. G. *J. Am. Chem. Soc.* **1980**, *102*, 4579.
(14) (a) Chisholm, M. H.; Cotton, F. A.; Extine, M. W.; Kelly, R. L. *J. Am. Chem. Soc.* **1979**, *101*, 7645. (b) Chisholm, M. H.; Hoffman, D. M.; Huffman, J. C. *Organometallics* **1985**, *4*, 986.

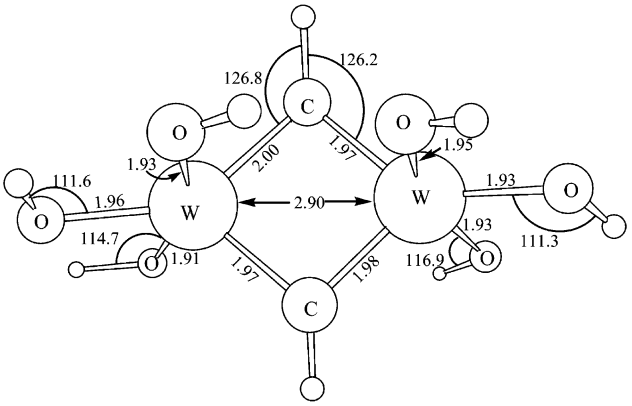

Figure 2. Optimized structure of $(HS)_3W(\mu\text{-}CH)_2W(SH)_3$ with selected bond lengths (Å) and angles (deg).

Table 1. Free Energy Values (kcal mol^{-1}) for the Reactions Involved in Acetylene Cleavage by Dinuclear $M_2(EH)_6$ Complexes, Where M = Mo, W and E = O, S

	Mo, O	Mo, S	W, O	W, S
$M_2(EH)_6 + HC{\equiv}H \rightarrow M_2(EH)_6(\mu\text{-}C_2H_2)$	4.5	−1.0	−0.8	−13.3
$M_2(EH)_6(\mu\text{-}C_2H_2) \rightarrow [(HE)_3M{\equiv}CH]_2$	5.0	21.0	−6.3	18.3
$M_2(EH)_6 + HC{\equiv}CH \rightarrow [(HE)_3M{\equiv}CH]_2$	9.5	20.0	−7.1	5.0

structure of $[(^tBuO)_3W{\equiv}CMe]_2$.[15] The bond lengths and angles of the optimized structure compare well with those of the actual molecule. The W−W nonbonding distances are 3.518(1) Å and 3.64 Å, and the W−C distances are 1.759(6) Å and 1.76 Å for the actual and model compounds, respectively. The observed and calculated W−O bond lengths are also quite similar, within 0.04 Å, with the longest W−O distances involving the bridging OH groups. The calculation of the model complex also reproduces the linearity of the W≡CH group with a calculated bond angle of 178.7°, compared to the actual bond angle of 179.8°. The W−O−C bond angles, 129.9(4)°−138.5(4)°, are larger than those in the model complex, 117.5°−126.2°, presumably because of the lack of steric bulk in the model compound. Using the "dimer" in the calculations has an additional advantage in that the second reaction, $M_2(OH)_6(\mu\text{-}C_2H_2)$ to $[(HE)_3M{\equiv}CH]_2$, can then be viewed as a unimolecular rearrangement. Calculations were also performed on molecules $(HE)_3M(\mu\text{-}CH)_2M(EH)_3$, where two alkylidyne groups bridge the two metals (Figure 2). These structures are over 15 kcal/mol higher in energy than those with terminal M≡C and bridging EH groups.

The geometries of all of the model compounds were optimized to minima in energy, and frequency calculations were performed to ensure that there were no imaginary frequencies.

The $\Delta G°$ values of the reactions shown in eq 5 at room temperature are given in Table 1. For the first step, the association of the alkyne with the dinuclear complex, the reaction is calculated to be more exergonic when E = S than when E = O and, for the hydroxide complexes, adduct formation for M = W is more thermodynamically favored than that for M = Mo. For the second step, rearrangement to the alkylidyne species, for M = W and E = O, the reaction is thermodynamically favored; $\Delta G° = -6$ kcal/mol, while, for M = Mo and E = O, $\Delta G°$ is calculated to be +5 kcal/mol. Experimentally,

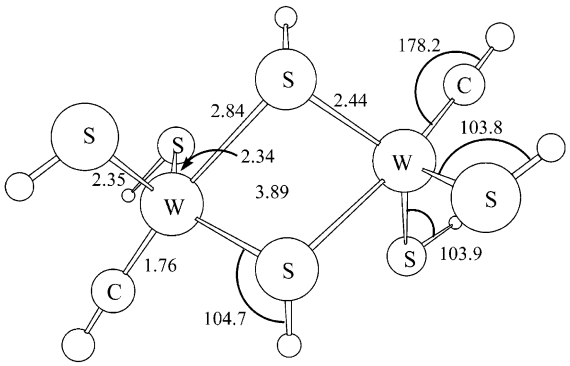

Figure 3. Optimized structure of $[W(\equiv CH)(SH)_3]_2$ with selected bond lengths (Å) and angles (deg).

$W_2(O^tBu)_6$ is known to readily react with alkynes in a quantitative manner to give alkylidyne complexes, while $Mo_2(O^tBu)_6$ only reacts with terminal alkynes under more forcing conditions to give low yields of $(^tBuO)_3Mo{\equiv}CR$.

For both metals, the reaction when E = S is considerably unfavorable, with a $\Delta G°$ of +21 kcal/mol for Mo and +18 kcal/mol for W. The optimized structures of the alkylidynes where E = S are somewhat different from those where E = O in that the M≡CH groups and bridging EH groups are no longer coplanar. This leads to more distorted pseudotrigonal bipyramidal coordination about the metal ions in the thiolates (Figure 3).

In addition to the thermodynamics of the system, we wished to gain an understanding of how the reaction proceeds and the height of the barriers of the reactions. We focused on the unimolecular rearrangement of the alkyne-adduct to the alkylidyne product and confined our study to E = O, as this reaction is not seen experimentally for E = S for either metal.

Transition State Study of $M_2(OH)_6(\mu\text{-}C_2H_2) \rightarrow [(HO)_3M{\equiv}H]_2$. In the reaction from $M_2(OH)_6(\mu\text{-}C_2H_2)$ to $[(HO)_3M{\equiv}CH]_2$, two M−C bonds, an M−M bond and a C−C bond, must be cleaved and M≡C triple bonds must be formed from single bonds. In addition, there is significant rearrangement necessary to place the carbon atoms *anti* to each other and to increase the M−M distance by approximately 1.1 Å. At the start, we imagined two ways in which these transformations could occur: (1) the carbon atoms could initially move away from each other in the direction of forming a planar M_2C_2 unit (**IV**), a 1,3-dimetallacyclobutadiene,[16] or (2) the C−C axis could initially rotate, as in the transformation of a dimetalatetrahedrane to a 1,2-dimetallocyclobutadiene (**V**).[17]

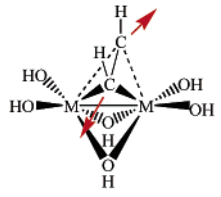

IV

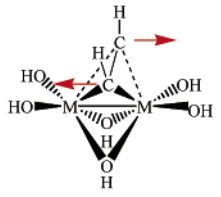

V

Calculated Reaction Coordinate for Molybdenum. The calculated reaction coordinate for $Mo_2(OH)_6(\mu\text{-}C_2H_2) \rightarrow [Mo(\equiv CH)(OH)_3]_2$ is given in terms of free energy in Figure 4,

(15) Chisholm, M. H.; Hoffman, D. M.; Huffman, J. C. *Inorg. Chem.* **1983**, *22*, 2903.

(16) Chisholm, M. H.; Heppert, J. A. *Adv. Organomet. Chem.* **1986**, *124*, 2697.
(17) Hoffman, D. M.; Hoffmann, R.; Fisel, C. R. *J. Am. Chem. Soc.* **1982**, *104*, 4, 3858.

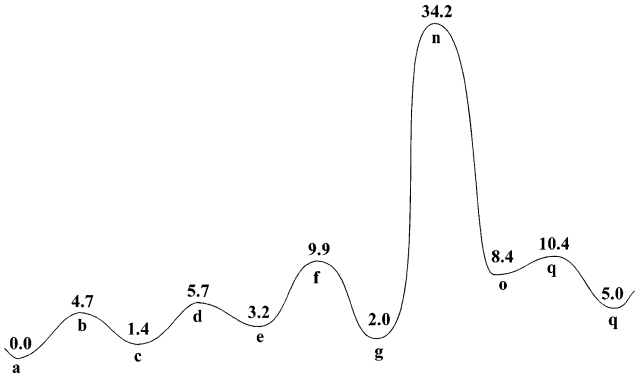

Figure 4. Reaction coordinate for $Mo_2(EH)_6(\mu\text{-}C_2H_2) \rightarrow [(HE)_3Mo{\equiv}CH]_2$ with free energy values (kcal mol^{-1}) given relative to $Mo_2(EH)_6(\mu\text{-}C_2H_2)$.

and energies and selected bond lengths of the species are given in Table 2. The transition state and intermediate structures along the pathway are shown and labeled **a**−**g** and **n**−**q**. Alternative views of some of these structures are given for clarity in the Supporting Information.

The highest lying transition state structure calculated for Mo, **n**, has one CH group terminal and the other CH group bridging the two metals. This structure is 34 kcal/mol higher in energy than $Mo_2(OH)_6(\mu\text{-}C_2H_2)$, **a**. In going from **a** to **n**, one M−C bond shortens from 2.10 to 1.79 Å, while the other M−C bond of the bridging CH group shortens from 2.09 to 1.87 Å. The M−M bond lengthens by approximately 0.1 Å. There is no longer a C−C bond in the transition state structure, and the C−C distance is 1.98 Å. The imaginary frequency for **n** moves the CH groups apart and together, and the latter leads to the reformation of the C−C bond.

The transition state **n** connects, in the forward direction, to a minimum (**o**) that is similar in structure to the alkylidyne product, $[Mo(\equiv CH)(OH)_3]_2$, except that the CH groups are not *anti* to each other. The M−M nonbonding distance is also somewhat shorter in **o** as compared to $[Mo(\equiv CH)(OH)_3]_2$ (**q**), with distances of 3.58 and 3.65 Å, respectively. The minimum **o** is 3 kcal/mol higher in energy than $[Mo(\equiv CH)(OH)_3]_2$. Another transition state, **p**, 2 kcal/mol higher than **o**, is required to connect the minima **o** and **q**.

The reaction coordinate from the high-lying transition state (**n**) to the reactant, $Mo_2(OH)_6(\mu\text{-}C_2H_2)$, is more complicated. In this direction, **n** connects to a minimum, **g**, in which the C−C axis is rotated approximately 45° to the Mo−Mo axis. The structure is 2 kcal/mol higher in energy than **a**, $Mo_2(OH)_6(\mu\text{-}C_2H_2)$. In the minimum **g**, the C−C bond is reformed and has a distance of 1.48 Å. Each CH group bonds to only one metal center, with relatively short Mo−C bond distances of 1.88 and 1.99 Å as compared to those of **a**, in which the Mo−C distances are 2.1 Å. Another transition state, **f**, returns the C−C axis perpendicular to the M−M axis and connects to a minimum, **e**, which is structurally very similar to $Mo_2(OH)_6(\mu\text{-}C_2H_2)$, except that two of the terminal OH groups have different orientations. Energetically, **e** is 3 kcal/mol higher than the reactant **a**. A transition state is needed to rotate each OH group back to the orientation in **a**. The first transition state, **d**, has an energy of 2.5 kcal/mol above that of **e** and leads to a minimum, **c**, which is only 1.4 kcal/mol above **a**. The last transition state required to connect to $Mo_2(OH)_6(\mu\text{-}C_2H_2)$, **b**, is 3.2 kcal/mol higher in energy than **c**.

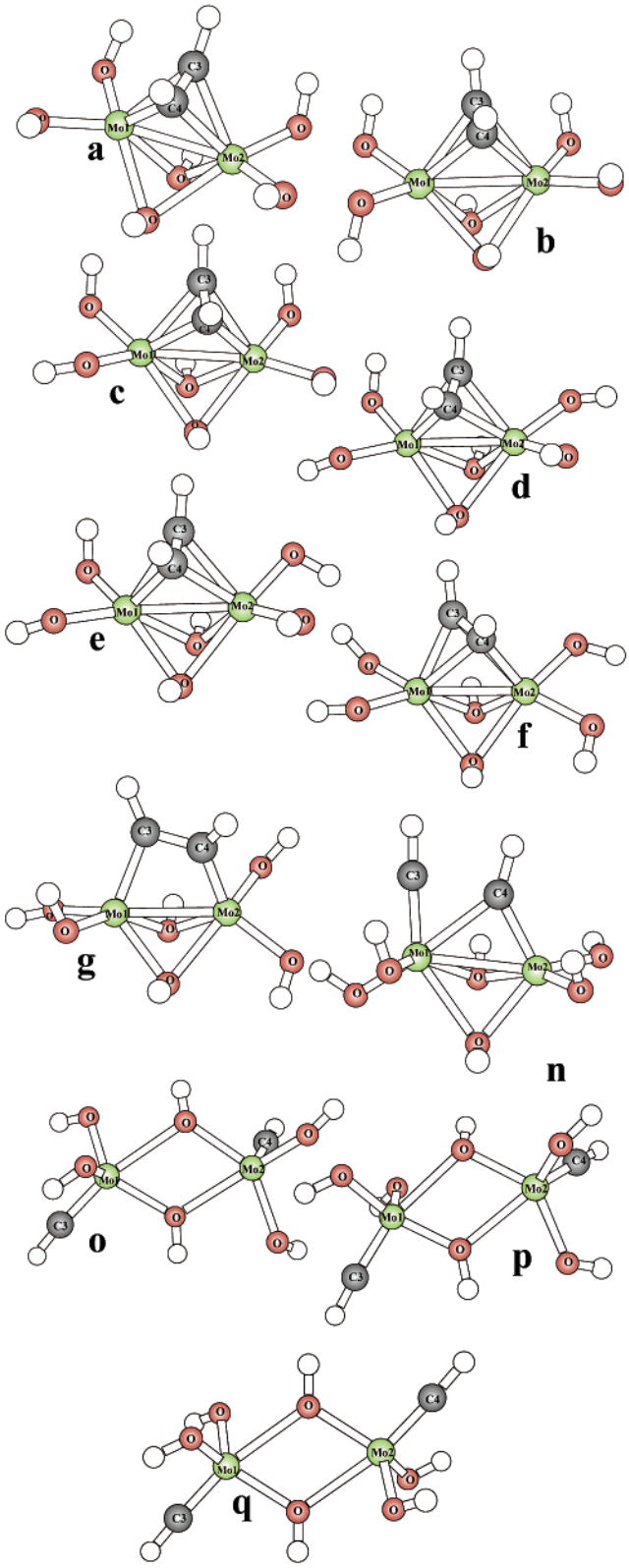

The transition state **n** is on a pathway between $Mo_2(OH)_6(\mu\text{-}C_2H_2)$ and $[Mo(\equiv CH)(OH)_3]_2$ that can be connected through a series of transition states and minima. Despite the complexity of the reaction coordinate, only the transition state **n** with a 34 kcal/mol activation energy is kinetically significant, as the other transition states occur at much lower energy. A graph of selected bond lengths plotted throughout the course of the reaction is

Table 2. Free Energies (kcal mol^{-1}) and Selected Bond Distances (Å) for Intermediates and Transitions States on the Mo Reaction Coordinate

	energy[a]	M–M	C–C	M1–C3	M1–C4	M2–C4	M2–C3	M1–O[b]	M1–O[c]	M2–O[b]	M2–O[c]
a	0.0	2.55	1.39	2.10	2.09	2.09	2.10	1.94	2.11	1.94	2.21
								1.92	2.21	1.92	2.11
b	4.7	2.56	1.39	2.11	2.08	2.10	2.10	1.94	2.07	1.94	2.20
								1.94	2.23	1.91	2.15
c	1.4	2.55	1.38	2.09	2.09	2.08	2.12	1.94	2.11	1.94	2.12
								1.94	2.20	1.91	2.21
d	5.7	2.54	1.40	2.10	2.08	2.09	2.07	1.93	2.19	1.96	2.19
								1.94	2.14	1.93	2.11
e	3.2	2.55	1.38	2.08	2.09	2.08	2.12	1.94	2.19	1.95	2.20
								1.93	2.13	1.92	2.12
f	9.9	2.48	1.39	1.97	2.31	2.00	2.43	1.95	2.14	1.93	2.12
								1.94	2.18	1.94	2.15
g	2.0	2.58	1.48	1.88	2.27	1.99	3.14	1.91	2.22	1.95	2.03
								1.97	2.06	1.90	2.26
n	34.2	2.66	1.98	1.79	2.27	1.87	3.44	1.92	2.33	1.91	2.05
								1.94	2.16	1.92	2.22
o	8.4	3.58	5.71	1.75	4.44	1.73	4.95	1.91	1.99	1.95	2.04
								1.92	2.36	1.91	2.26
p	10.4	3.61	6.09	1.75	4.70	1.73	4.99	1.91	1.98	1.95	2.03
								1.92	2.38	1.91	2.32
q	5.0	3.65	6.67	1.74	5.09	1.74	5.09	1.92	1.97	1.92	1.97
								1.92	2.42	1.92	2.43

[a] Relative to **a** (the absolute energy of **a** is −667.424 659 Hartree). [b] Terminal. [c] Bridge.

Table 3. Free Energies (kcal mol^{-1}) and Selected Bond Distances[d] (Å) for Intermediates and Transitions States on the W Reaction Coordinate

	energy[a]	M–M	C–C	M1–C3	M1–C4	M2–C4	M2–C3	M1–O[b]	M1–O[c]	M2–O[b]	M2–O[c]
A	6.3	2.58	1.44	2.08	2.08	2.08	2.08	1.92	2.13	1.92	2.13
								1.91	2.19	1.91	2.19
B	11.6	2.58	1.45	2.09	2.06	2.09	2.06	1.92	2.11	1.92	2.18
								1.94	2.19	1.91	2.17
C	8.4	2.57	1.44	2.07	2.07	2.07	2.10	1.93	2.13	1.92	2.20
								1.93	2.17	1.91	2.13
D	11.3	2.57	1.45	2.07	2.07	2.07	2.06	1.92	2.15	1.94	2.13
								1.94	2.17	1.92	2.16
E	10.1	2.57	1.45	2.06	2.08	2.06	2.08	1.92	2.17	1.93	2.14
								1.93	2.14	1.92	2.17
F	14.6	2.52	1.43	1.96	2.25	1.99	2.35	1.94	2.14	1.92	2.11
								1.94	2.16	1.93	2.18
G	6.2	2.54	1.44	1.95	2.57	1.96	2.62	1.91	2.21	1.94	2.06
								1.96	2.07	1.90	2.26
H	12.9	2.56	1.44	1.95	2.55	1.95	2.65	1.92	2.22	1.95	2.04
								1.96	2.06	1.91	2.25
I	8.4	2.54	1.44	1.95	2.60	1.95	2.59	1.91	2.22	1.95	2.06
								1.95	2.06	1.91	2.22
J	21.8	2.64	1.50	1.86	2.26	1.99	3.12	1.92	2.14	1.93	2.11
								1.93	2.46	1.92	1.98
K	19.8	2.62	1.45	1.88	2.20	2.03	3.21	1.91	2.13	1.94	2.17
								1.92	(3.02)	1.93	(1.92)
L	23.1	2.61	1.47	1.88	2.20	2.01	3.21	1.91	2.12	1.92	2.19
								1.92	(2.91)	1.94	(1.93)
M	18.3	2.61	1.46	1.88	2.20	2.02	3.21	1.91	2.12	1.92	2.21
								1.93	(2.99)	1.92	1.93
N	25.4	2.63	1.89	1.81	2.24	1.89	3.39	1.92	2.16	1.90	2.18
								1.93	2.34	1.91	2.05
O	2.6	3.56	5.70	1.77	4.43	1.74	4.96	1.90	1.99	1.93	2.04
								1.91	2.34	1.90	2.23
P	5.4	3.61	6.23	1.76	4.78	1.75	5.02	1.90	1.98	1.94	2.02
								1.91	2.35	1.90	2.30
Q	0.0	3.64	6.70	1.76	5.10	1.76	5.10	1.91	1.97	1.91	1.97
								1.91	2.40	1.91	2.40

[a] Relative to **Q** (the absolute energy of **Q** is −668.059 904 Hartree). [b] Terminal. [c] Bridge. [d] Bond lengths in parentheses are for species in which the W−O−W bridge has opened.

given in Figure 5, which shows that large changes in bond length occur around the high-lying transition state, **n**. Throughout the course of the reaction, the Mo−O distances also change considerably. The terminal O−Mo bond distances range from 1.90 to 1.97 Å, while the bridging O−Mo bond lengths range from 2.03 to 2.42 Å.

Calculated Reaction Coordinate for Tungsten. The calculated reaction coordinate for $W_2(OH)_6(\mu\text{-}C_2H_2) \rightarrow [W(\equiv CH)(OH)_3]_2$ is given in terms of free energy in Figure 6, and energies and selected bond lengths of the species are given in Table 3.

For tungsten, the overall reaction coordinate is more complicated with additional minima and transition states. Still, many

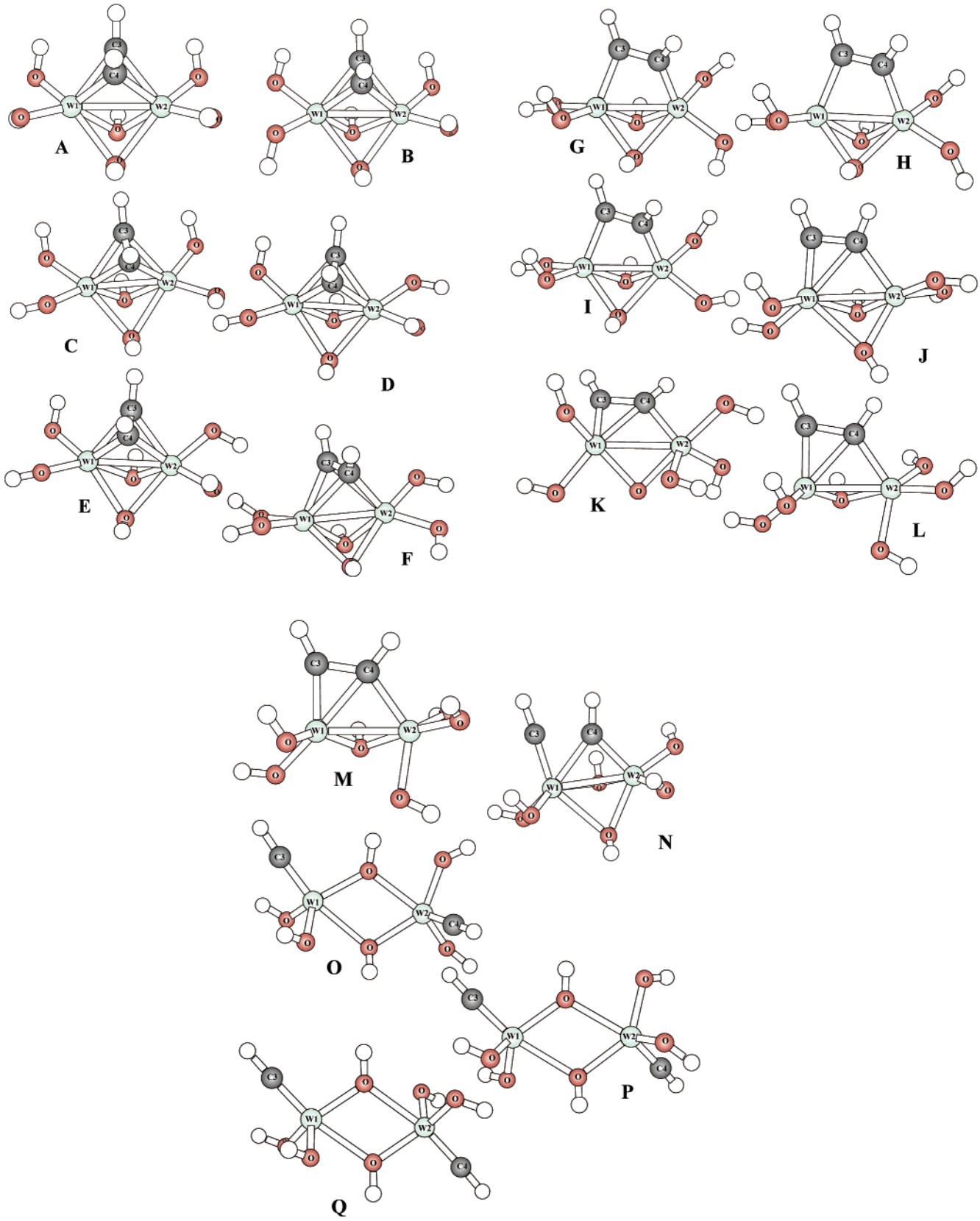

of the transition states and minimum energy structures have essentially the same geometries as those for Mo, and therefore the same letters, **A**−**Q**, are used to denote similar structures for ease of comparison. Some of the structures are again shown from a different viewpoint in the Supporting Information to give a clearer picture of the molecular geometry.

The highest-lying transition state for the reaction, **N**, is very similar in geometry to that of Mo, with one bridging and one terminal CH group. In this case, however, **N** is only 19 kcal/mol higher in energy than **A**, $W_2(OH)_6(\mu\text{-}C_2H_2)$. The transition state **N** again has a longer M−M distance than that of **A** (2.63 Å vs 2.58 Å), and the C−C bond has been broken. The terminal

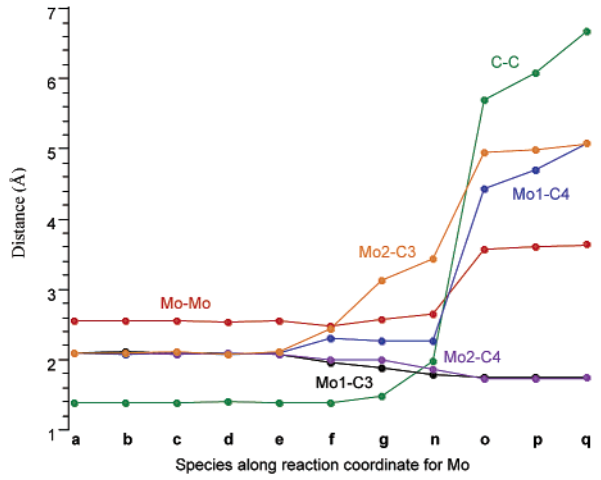

Figure 5. Selected bond lengths during the course of $Mo_2(EH)_6(\mu\text{-}C_2H_2) \rightarrow [(HE)_3Mo{\equiv}CH]_2$.

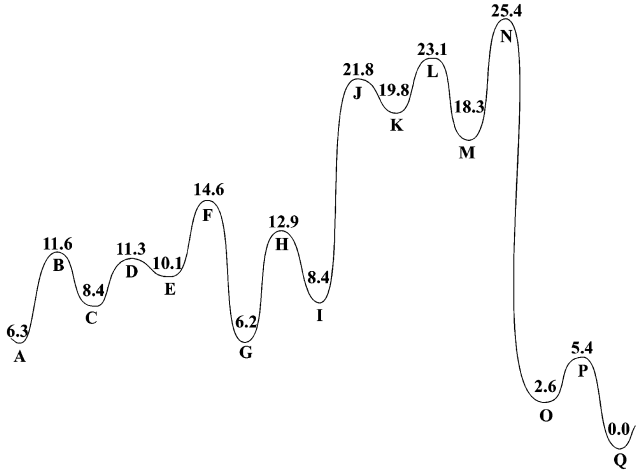

Figure 6. Reaction coordinate for $W_2(EH)_6(\mu\text{-}C_2H_2) \rightarrow [(HE)_3W{\equiv}CH]_2$ with free energy values (kcal mol^{-1}) given relative to $[(HE)_3W{\equiv}CH]_2$.

M−C distance is 1.81 Å, while the bridging group has M−C distances of 1.89 and 2.24 Å, comparable to double and single bonds, respectively.

In the forward direction from **N**, the pathway is basically the same as that for Mo. **N** leads to a minimum **O** that is 3 kcal/mol higher in energy than $[W(\equiv CH)(OH)_3]_2$ (**Q**). Once again, the main difference between **O** and **Q** is the disposition of the CH groups. The transition state **P** connects the two minima and occurs approximately 2 kcal/mol higher in energy than that of **O**.

In the reverse direction, **N** leads to a minimum, **M**, in which the C−C bond has reformed, shortening from 1.89 Å in **N** to 1.46 Å in **M**. In this structure, one of the OH bridges has also opened, resulting in 5 terminal OH groups. The reaction coordinate goes through 2 transition states (**L** and **I**) and another minimum energy structure (**K**) before the OH bridge is closed again. **K** has a very similar geometry to that of **M**, although a terminal OH group has been rotated and **K** is higher energetically by almost 2 kcal/mol. The transition state connecting these structures is 5 kcal/mol higher in energy than **M**. **K** connects through the transition state **J**, with a barrier of 2 kcal/mol, to the minimum **I** which is 12 kcal/mol lower than **K**. The C−C axis is rotated approximately 45° to the W−W axis in the minimum structure **I**. The C−C bond length is 1.44 Å, the same as that in $W_2(OH)_6(\mu\text{-}C_2H_2)$, and the M−C bond lengths are 1.95 Å, which is roughly 0.13 Å shorter than those in $W_2(OH)_6(\mu\text{-}C_2H_2)$. Another transition state with a barrier of 5 kcal/mol is required to rotate about a W−OH bond to give **G**, which is isostructural with **g** for molybdenum. This minimum is 2 kcal/mol lower than **I**. The rest of the reaction coordinate is essentially the same as that for Mo. The next transition state connects to a minimum in which the C−C axis is again perpendicular to the W−W axis. Two transition states are then required to move the terminal OH groups into the same orientation as that in $W_2(OH)_6(\mu\text{-}C_2H_2)$.

Table 4. Mulliken Charges of Reactant, Transitions States, Intermediates, and Product for M = Mo and W

W	M1	M2	C3	C4	Mo	M1	M2	C3	C4
A	1.27	1.27	−0.43	−0.43	**a**	1.19	1.19	−0.39	−0.37
B	1.29	1.25	−0.44	−0.43	**b**	1.21	1.17	−0.39	−0.37
C	1.26	1.27	−0.43	−0.42	**c**	1.18	1.19	−0.39	−0.36
D	1.28	1.30	−0.44	−0.45	**d**	1.20	1.22	−0.40	−0.39
E	1.28	1.28	−0.43	−0.43	**e**	1.17	1.19	−0.38	−0.36
F	1.25	1.26	−0.39	−0.44	**f**	1.17	1.17	−0.33	−0.39
G	1.2	1.24	−0.36	−0.38	**g**	1.13	1.17	−0.34	−0.36
H	1.19	1.28	−0.37	−0.37					
I	1.22	1.22	−0.37	−0.37					
J	1.23	1.34	−0.37	−0.52					
K	1.18	1.33	−0.38	−0.54					
L	1.22	1.29	−0.39	−0.52					
M	1.21	1.28	−0.38	−0.52					
N	1.26	1.23	−0.41	−0.47	**n**	1.18	1.14	−0.36	−0.45
O	1.28	1.22	−0.41	−0.35	**o**	1.21	1.15	−0.36	−0.32
P	1.27	1.23	−0.4	−0.37	**p**	1.20	1.16	−0.35	−0.34
Q	1.27	1.27	−0.41	−0.41	**q**	1.19	1.19	−0.36	−0.36

Despite the additional complexity of the reaction coordinate for tungsten, the highest-lying transition state is still **N** with a barrier of 19 kcal/mol. This is 15 kcal/mol lower than the **n** energy barrier for molybdenum. At ambient temperatures, it would be thermally accessible and would therefore allow the reaction to occur in the case of tungsten, but for molybdenum, the greater barrier would prevent the reaction, even if the alkylidyne was thermodynamically favored.

For both metals, a significant portion of the calculated reaction coordinate involves rotation of the OH groups. These rotations are calculated to have low barriers for the model compounds and would occur readily at room temperature. However, steric bulk in the actual alkoxide complexes would influence the height of these rotational barriers.

Mulliken Charges. The Mulliken charges for the intermediate and transition state structures along the pathway from $M_2(OH)_6(\mu\text{-}C_2H_2)$ to $[M(\equiv CH)(OH)_3]_2$ are given in Table 4. It is interesting to note that there are very small changes in the Mulliken charges on the metal atoms and the alkyne/alkylidyne carbons throughout the course of the reaction. This lack of variation contrasts with the formal oxidation states of +5 and +6 assignable to the metal atoms in the dimetalatetrahedrane and methylidyne complexes, respectively.

Concluding Remarks

DFT calculations on the thermodynamics and kinetics of the alkyne cleavage reactions lead to a better understanding of the effects of the ancillary ligands and the metals, Mo versus W, on the Schrock "chop-chop" reaction. The observed reduced activity of $Mo_2(O^tBu)_6$ complexes to alkyne cleavage can be seen to arise from the significantly higher barrier to the reaction.

Moreover for the model compounds with hydroxide ligands, the metathesis reaction leading to the methylidyne ligands is thermodynamically unfavorable.

In 1995, Morokuma and co-workers[18] reported the activation energy calculated for the cleavage of dinitrogen by ML_3 complexes, where M = Mo, W and L = H, Cl and NH_2. They also found that the barrier for N_2 activation to be smaller for M = W compared to M = Mo (14.4 kcal/mol for Mo and 3.6 kcal/mol for W). Experimentally, dinitrogen cleavage is seen with $Mo(NRAr)_3$, where $R = C(CD_3)_2CH_3$ and Ar = 3,5-$C_6H_3Me_2$.

There are some interesting similarities and differences in the reaction pathway involving the reductive cleavage of N_2 and C_2H_2 by mononuclear L_3Mo and dinuclear M_2L_6 species. In the reactions involving the MoL_3 compounds and dinitrogen, there is a stepwise formation of linear $L_3Mo(\mu\text{-}N_2)MoL_3$ species which is followed by a rate-determining N−N cleavage involving a nonlinear transition state depicted by **VI**.

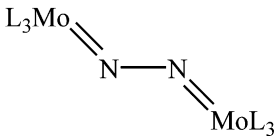

VI

The microscopic reverse, the formation of the N−N bond in the coupling of two M≡N groups, can be viewed similarly. When the two metal fragments are not the same, one nucleophilic nitride may attack the M−N π^* orbital of another. In the case of the dinuclear M_2L_6 compounds, cleavage of the C≡C bond must also occur with M−M bond cleavage. Our calculations implicate a rather unsymmetrical transition state. There is some similarity in the zigzag M−C−C−M bridge with the M−N−N−M bridge, although the atoms in the former do not lie in a plane. Moreover, our calculations reveal the rather intricate role of the bridging OH groups that persist throughout the reaction. There is no evidence that amido bridges are involved in the Cummins' scission of dinitrogen. Clearly, though the two systems are similar, there are significant differences that arise from reactions involving mononuclear metal fragments and those wherein the starting material is dinuclear and has a metal−metal multiple bond.

Further studies are planned, including a theoretical investigation into the reductive cleavage of nitriles by metal−metal triply bonded compounds.

(18) Cui, Q.; Musaev, D. G.; Svensson, M.; Sieber, S.; Morokuma, K. *J. Am. Chem. Soc.* **1995**, *117*, 12366.

Computational Details

All calculations were performed with the Gaussian 98 package,[10] using the B3LYP[19] method. The LANL2DZ basis set[20] was used for the metals, and the 6-31G* basis set,[21] for oxygen, carbon, sulfur, and hydrogen. All stationary points were characterized as minima or transition states by frequency calculations. Frequency calculations were also used to obtain the free energy values.

To find transition states, the Z matrix of the reactant was distorted toward the product in 10 steps, with single point calculations performed at each step. The highest energy point was used as an initial guess for the transition state structure using QST3.[22] An IRC calculation[23] from the transition state structure, followed by further optimization and frequency calculations of the endpoints of the IRC calculation, determined the true minima that connected to each transition state.

Acknowledgment. We thank the National Science Foundation for funding through grant CHE-9982415 to Ernest Davidson.

Supporting Information Available: Alternative views of intermediate structures **e**−**g** for the $Mo(EH)_6(\mu\text{-}C_2H_2) \rightarrow [(HE)_3Mo{\equiv}CH]_2$ reaction coordinate and alternative views of intermediate structures **F**−**N** for the $W_2(EH)_6(\mu\text{-}C_2H_2) \rightarrow [(HE)_3W{\equiv}CH]_2$. This material is available free of charge via the Internet at http://pubs.acs.org.

JA020847Q

(19) Becke, A. D. *J. Chem. Phys.* **1993**, *98*, 5648.
(20) (a) Hay, P. J.; Wadt, W. R. *J. Chem. Phys.* **1985**, *82*, 270. (b) Wadt, W. R.; Hay, P. J. *J. Chem. Phys.* **1985**, *82*, 284. (c) Hay, P. J.; Wadt, W. R. *J. Chem. Phys.* **1985,** *82*, 299.
(21) (a) Ditchfield, R.; Hehre, W. J.; Pople, J. A. *J. Chem. Phys.* **1971**, *54*, 724. (b) Hehre, W. J.; Ditchfield, R.; Pople, J. A. *J. Chem. Phys.* **1972**, *56*, 2257. (c) Hariharan, P. C.; Pople, J. A. *Mol. Phys.* **1974**, *27*, 209. (d) Gordon, M. S. *Chem. Phys. Lett.* **1980**, *76*, 163. (e) Hariharan, P. C.; Pople, J. A. *Theor. Chim. Acta* **1973**, *28*, 213.
(22) (a) Peng, C.; Schlegel, H. B. *Isr. J. Chem.* **1993**, *33*, 449. (b) Peng, C.; Ayala, P. Y.; Schlegel, H. B.; Frisch, M. J. *J. Comput. Chem.* **1994**, *16*, 49.
(23) (a) Gonzalez, C.; Schelegel, H. B. *J. Chem. Phys.* **1989**, *90*, 2154. (b) Gonzalez, C.; Schelegel, H. B. *J. Phys. Chem.* **1990**, *94*, 5523.